PHILOSOPHICAL MAGAZINE, 21 March 2004
VOL. 84, NO. 9, 847–863

Taylor & Francis
Taylor & Francis Group

Yield stress of nanocrystalline materials: role of grain-boundary dislocations, triple junctions and Coble creep

M. YU. GUTKIN, I. A. OVID'KO†

Institute of Problems of Mechanical Engineering, Russian Academy of Sciences, Bolshoj 61, Vasil. Ostrov, St Petersburg 199178, Russia

and C. S. PANDE

Naval Research Laboratory, Washington, DC 20375, USA

[*Received 31 March 2003 and accepted in revised form 14 August 2003*]

ABSTRACT

A theoretical model is suggested which describes the strengthening of nanocrystalline materials due to the effects of triple junctions of grain boundaries as obstacles for grain-boundary sliding. In the framework of the model, a dependence of the yield stress characterizing grain-boundary sliding on grain size and triple-junction angles is revealed. With this dependence we have found that, in as-fabricated nanocrystalline materials, the yield stress depends upon a competition between conventional dislocation slip and grain-boundary sliding. On the other hand, yield stress dependence on grain size in heat-treated nanocrystalline materials is described as that caused by a competition between conventional dislocation slip and Coble creep. Grain-size and triple-junction angle distributions are incorporated into the consideration to account for distributions of grain size and triple-junction angles, occurring in real specimens. The results of the model are compared with experimental data from as-fabricated and heat-treated nanocrystalline materials and shown to be in good agreement.

§1. INTRODUCTION

Nanocrystalline materials exhibit unique mechanical properties which are different from those of conventional coarse-grained polycrystals (for example Koch *et al.* (1999), Mohamed and Li (2001) and Padmanabhan (2001)). This is related, in many aspects, to the effects of grain boundaries (GBs) whose volume fraction rapidly grows with grain refinement. In fact, high-density ensembles of GBs serve as obstacles for conventional dislocation slip in nanocrystalline materials and, at the same time, open up several effective deformation modes that usually are not significant in coarse-grained polycrystals. These modes are GB diffusional creep (Masumura *et al.* 1998, Kim *et al.* 2000, Yamakov *et al.* 2002), triple-junction diffusional creep (Fedorov *et al.* 2002), rotational mode (occurring via movement of GB disclinations) (Ke *et al.* 1995, Hackney *et al.* 1996, Gutkin *et al.* 2002, Murayama *et al.* 2002,

† Author for correspondence. Email: ovidko@def.ipme.ru.

Philosophical Magazine ISSN 1478–6435 print/ISSN 1478–6443 online © 2004 Taylor & Francis Ltd
http://www.tandf.co.uk/journals
DOI: 10.1080/14786430310001616063

Ovid'ko 2002) and GB sliding (Hahn *et al.* 1997, Hahn and Padmanabhan 1997, Konstantinidis and Aifantis 1998, Fedorov *et al.* 2003) (for a review, see Gutkin *et al.* (2001)). In these circumstances, grain refinement causes switching from conventional lattice dislocation slip to deformation modes conducted by GB dislocations, GB disclinations and point defects. The effective actions of various deformation modes that are in competition with each other are believed to cause the unique deformation behaviour of nanocrystalline materials.

The competition between different deformation modes in nanocrystalline materials is caused by their structural peculiarities which, in general, are sensitive to fabrication and processing technologies. Two nanocrystalline specimens with the same compositions and mean grain sizes, which are prepared by different procedures, may exhibit different mechanical properties (Koch *et al.* 1999, Mohamed and Li 2001, Padmanabhan 2001). In this context, the structure and geometry of triple junctions of GBs are among the most important issues for the mechanical behaviour of nanocrystalline materials. Indeed, in recent years, triple junctions have been recognized as defects with the structure and properties being different from those of the GBs that they adjoin (for example Gutkin and Ovid'ko (1994) and King (1999)). In particular, triple junctions serve as carriers of enhanced diffusional creep (Rabukhin 1986, Fedorov *et al.* 2002), sources of lattice dislocations (Owusu-Boahen and King 2001), and strengthening elements for GB sliding (Hahn *et al.* 1997, Hahn and Padmanabhan 1997, Konstantinidis and Aifantis 1998, Fedorov *et al.* 2003) in plastically deformed coarse- and fine-grained materials. As a corollary, triple junctions are structural elements that are capable of playing the important or even crucial role in the 'fabrication–structure–mechanical properties' relationship in namely nanocrystalline materials where the volume fraction of triple junctions is extremely high. The role of triple junctions as inherent structural elements of nanocrystalline materials should definitely be taken into consideration when discussing the specific features of deformation in nanocrystalline materials.

One such specific feature manifests itself in deviations from the conventional grain-size–strength relationship. More precisely, the dependence of the yield stress τ_y on grain size d deviates from the classical Hall–Petch relationship ($\tau_y = \tau_0 + kd^{-1/2}$, with τ_0 and k being constant parameters) at small d being of the order of 10 nm (Koch *et al.* 1999, Padmanabhan 2001). As has been experimentally detected by Weertman and Sanders (1994) and Volpp *et al.* (1997), the $\tau_y(d)$ dependence in nanocrystalline materials shows two different behaviours, depending on their mode of processing. In the range of small grain sizes, heat-treated materials exhibit 'inverse' Hall–Petch behaviour (softening with reduction in grain size), while the yield stress or hardness of as-prepared materials slightly increases or saturates at grain size $d \leqslant 10$ nm (Weertman and Sanders 1994, Volpp *et al.* 1997) showing little or no 'inverse' Hall–Petch behaviour. We think that this difference between the deformation behaviours of heat-treated and as-prepared nanocrystalline materials is related to the difference between their defect structures. Different defect structures in heat-treated and as-prepared materials cause the occurrence of effective action of different deformation modes owing to grain refinement. In particular, the contribution of GB sliding is expected to be high in as-prepared materials commonly characterized by high density of lattice and GB dislocations which enhance GB sliding processes. On the other hand, heat treatment is capable of suppressing the GB sliding, in which case other deformation modes effectively come into play. We present a theoretical model describing GB sliding and its contribution to plastic

flow in both as-prepared and heat-treated nanocrystalline materials. In doing so, special attention will be paid to the role of triple junctions of GBs in GB sliding processes in nanocrystalline materials.

§ 2. Grain-boundary dislocations and triple junctions in plastically deformed nanocrystalline materials

Let us consider a nanocrystalline specimen fabricated in highly non-equilibrium conditions. Most of the fabrication routes produce highly defective GBs. In particular, GBs with an excess density of GB dislocations (carriers of GB sliding) often exist in as-fabricated nanocrystalline materials (Valiev and Alexandrov 2000, Mohamed and Li 2001) (figure 1 (*a*)). When a mechanical load is applied to the specimen, mobile GB dislocations (with the Burgers vector being parallel to GB planes) move, causing GB sliding. Some moving GB dislocations annihilate with GB dislocations having Burgers vectors of opposite sign (figure 1 (*b*)). Other GB dislocations are stopped at triple junctions of GBs, which represent effective obstacles for dislocation movement (figure 1 (*b*)). In general, GB dislocations stopped near a triple junction are capable of overcoming the junction obstacle by a dislocation reaction when the shear stress reaches some critical value. In nanocrystalline materials with their high-density ensembles of triple junctions, the critical shear stress needed for GB dislocations to overcome triple junctions specifies the contribution of GB sliding to the yield stress. In these circumstances, the critical shear stress is a very important parameter of plastic deformation in nanocrystalline materials,

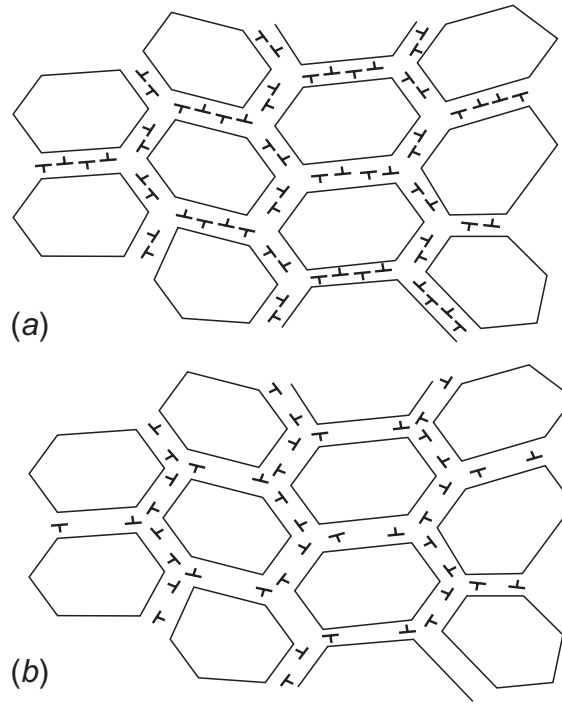

Figure 1. GB dislocation ensemble in an as-prepared nanocrystalline specimen (*a*) before and (*b*) after mechanical load.

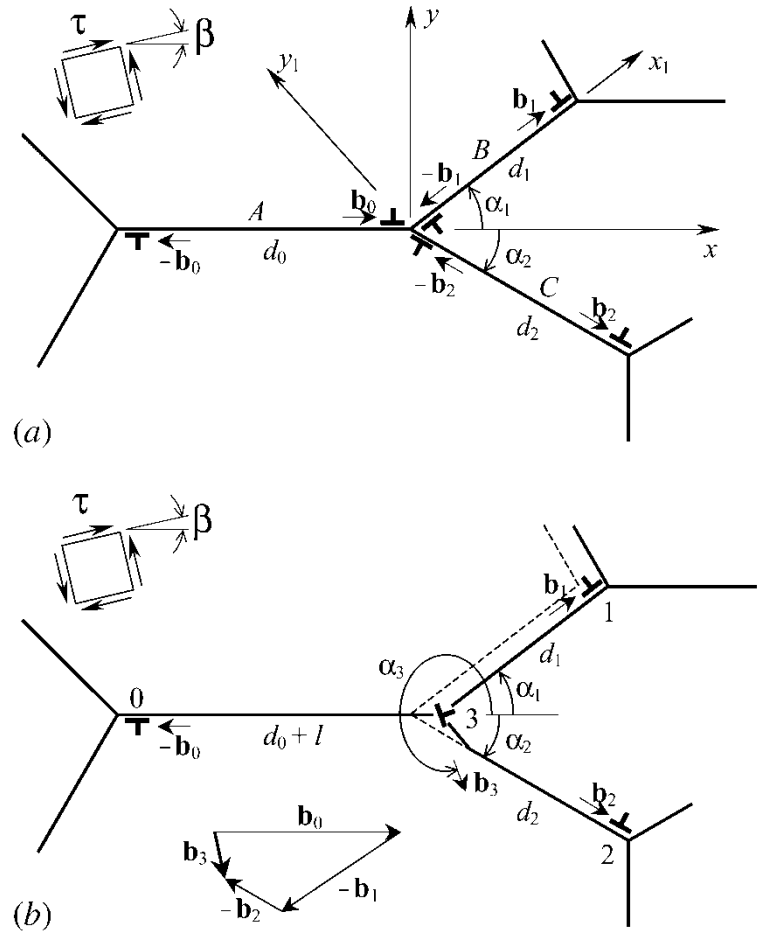

Figure 2. Elementary act of GB sliding in mechanically loaded nanocrystalline specimen. (*a*) GB dislocations are accumulated near triple junctions. (*b*) A dislocation with Burgers vector $\mathbf{b}_0$ transfers by a distance l, in which case it comes into reaction with two dislocations (with Burgers vectors $-\mathbf{b}_1$ and $-\mathbf{b}_2$), resulting in the formation of a GB dislocation with Burgers vector $\mathbf{b}_3$.

which quantitatively characterizes GB sliding as a deformation mode being in competition with other deformation modes.

The main aim of this paper is to calculate the critical shear stress in question in the framework of the model described below. We consider a model configuration of GB dislocations in a nanocrystalline material, which is formed near a triple junction under the action of shear stress τ (figure 2(*a*)). The configuration consists of three dipoles of GB dislocations with Burgers vectors $\pm\mathbf{b}_0$, $\pm\mathbf{b}_1$ and $\pm\mathbf{b}_2$, which are parallel to the corresponding GB planes adjacent to the triple junction. GB dislocations are stopped by the (central) triple junction and its neighbouring triple junctions (figure 2(*a*)), in which case the interspacings between the GB dislocations that form the three dipole configurations are tentatively equal to the corresponding GB lengths d_0, d_1 and d_2 respectively. Let us designate the GB dislocation dipoles as A, B and C, respectively. In our consideration, we assume that energy barriers for GB

dislocations to overcome triple junctions are all different, but the lowest barrier characterizes the central triple junction. With this assumption, in order to estimate the yield stress for GB sliding, we should analyse the energy chracteristics of transformations of GB dislocations, occurring at the central triple junction. In doing this, we note that an elementary act of the GB sliding is a transfer of the GB dislocation with Burgers vector $\mathbf{b}_0$ (initially stopped by the central triple junction at GB of length d_0) to the neighbouring GB of length d_2. This transfer over a short distance l occurs at critical shear stress τ_c at which the transfer becomes energetically favourable. The transfer is accompanied by a dislocation reaction which involves all the three GB dislocations stopped at the central triple junction and results in the formation of a sessile GB dislocation with Burgers vector $\mathbf{b}_3 = \mathbf{b}_0 - \mathbf{b}_1 - \mathbf{b}_2$ (figure 2 (*b*)). The process discussed is an elementary relaxation process contributing to plastic deformation of a nanocrystalline specimen under a mechanical load. It is characterized by the shear stress τ_c which, in the framework of our model, specifies the contribution of GB sliding to the yield stress of a nanocrystalline material. The stress τ_c essentially depends on characteristics of GB dislocations and the central triple junction. In order to reveal these dependences, we shall calculate below the difference between energies of the final (figure 2 (*b*)) and the initial (figure 2 (*a*)) configurations of defects in a plastically deformed nanocrystalline material.

§ 3. Yield stress for grain-boundary sliding in nanocrystalline materials

The initial defect configuration (figure 2 (*a*)) is characterized by the total energy density (per unit of GB dislocation length) W_1^t which consists of six key terms:

$$W_1^t = W_A + W_B + W_C + W_{AB} + W_{AC} + W_{BC}. \tag{1}$$

Here W_A, W_B and W_C are the proper energy densities of GB dislocation dipoles A, B and C, respectively. W_{AB}, W_{AC} and W_{BC} are the energy densities that characterize the elastic interactions between GB dislocation dipoles A and B, A and C, and B and C, respectively.

The proper energy density of a dislocation dipole is effectively calculated as the work spent to the generation of the dipole in its stress field. Such calculations are, in fact, routine and may be found in literature (for example Gutkin and Ovid'ko (2001)). Following these calculations, the energy densities of GB dislocation dipoles are as follows:

$$W_A = Db_0^2\left[\ln\left(\frac{d_0}{r_{c0}}\right) + Z_0\right], \tag{2}$$

$$W_B = Db_1^2\left[\ln\left(\frac{d_1}{r_{c1}}\right) + Z_1\right], \tag{3}$$

$$W_C = Db_2^2\left[\ln\left(\frac{d_2}{r_{c2}}\right) + Z_2\right]. \tag{4}$$

Here $D = G/2\pi(1-\nu)$, G is the shear modulus, ν Poisson's ratio, $r_{c0} \approx r_{c1} \approx r_{c2} = r_c$ are the dislocation core radii, and $Z_0 \approx Z_1 \approx Z_2 = Z$ are the factors for taking

into account the contributions of dislocation cores into the energy density. The characteristic value of r_c is of the order of the magnitude of the Burgers vector which is in the range 0.08–0.1 nm for a GB dislocation (Sutton and Balluffi 1995). The dipole arms are larger than a few nanometres. Hence the above energy formulas should be quite accurate for our first-approximation model.

Now let us calculate the energy densities W_{AB}, W_{AC} and W_{BC}. The energy density that characterizes the interaction between two GB dislocation dipoles can be effectively calculated as the work spent in generating one dipole in the stress field of another dipole (Mura 1968). For instance, the energy density W_{AB} that characterizes the elastic interaction between GB dislocation dipoles A and B is given by the following formula:

$$W_{AB} = -b_0 \int_{-d_0}^{-r_c} \sigma_{xy}^{(1)}(x, y = 0)\, dx, \tag{5}$$

where $\sigma_{xy}^{(1)}$ is the xy component of the stress field created by the dipole B. In general, the stress field $\sigma_{xy}^{(1)}(x, y)$ is as follows:

$$\sigma_{xy}^{(1)}(x, y) = \left(\sigma_{x_1x_1}^{(1)} - \sigma_{y_1y_1}^{(1)}\right) \sin\alpha_1 \cos\alpha_1 + \sigma_{x_1y_1}^{(1)} \cos(2\alpha_1), \tag{6}$$

where the stress field components $\sigma_{x_1x_1}^{(1)}$, $\sigma_{y_1y_1}^{(1)}$ and $\sigma_{x_1y_1}^{(1)}$ are written in the coordinate system (x_1, y_1) (see figure 2). These components are given by the known formulae (Hirth and Lothe 1982)

$$\sigma_{x_1x_1}^{(1)} = Db_1y_1\left(\frac{3x_1^2 + y_1^2}{(x_1^2 + y_1^2)^2} - \frac{3(x_1 - d_1)^2 + y_1^2}{[(x_1 - d_1)^2 + y_1^2]^2}\right), \tag{7}$$

$$\sigma_{y_1y_1}^{(1)} = Db_1y_1\left(-\frac{x_1^2 - y_1^2}{(x_1^2 + y_1^2)^2} + \frac{(x_1 - d_1)^2 - y_1^2}{[(x_1 - d_1)^2 + y_1^2]^2}\right), \tag{8}$$

$$\sigma_{x_1y_1}^{(1)} = Db_1\left(-\frac{x_1(x_1^2 - y_1^2)}{(x_1^2 + y_1^2)^2} + \frac{(x_1 - d_1)[(x_1 - d_1)^2 - y_1^2]}{[(x_1 - d_1)^2 + y_1^2]^2}\right), \tag{9}$$

where coordinates (x_1, y_1) are in the following relationships with coordinates (x, y):

$$x_1 = x\cos\alpha_1 + y\sin\alpha_1, \tag{10}$$

$$y_1 = y\cos\alpha_1 - x\sin\alpha_1. \tag{11}$$

With equations (7)–(11), substitution of equation (6) into equation (5) gives the interaction energy density

$$W_{AB} = -Db_0b_1\left[\frac{\cos\alpha_1}{2}\ln\left(\frac{d_0^2d_1^2}{r_c^2(d_0^2 + 2d_0d_1\cos\alpha_1 + d_1^2)}\right) + \frac{d_0d_1\sin^2\alpha_1}{d_0^2 + 2d_0d_1\cos\alpha_1 + d_1^2}\right]. \tag{12}$$

By analogy with the calculation scheme for W_{AB}, we calculate the interaction energy densities W_{AC} and W_{BC} which are respectively as follows:

$$W_{AC} = -Db_0b_2\left(\frac{\cos\alpha_2}{2}\ln\left(\frac{d_0^2d_2^2}{r_c^2(d_0^2+2d_0d_2\cos\alpha_2+d_2^2)}\right)+\frac{d_0d_2\sin^2\alpha_2}{d_0^2+2d_0d_2\cos\alpha_2+d_2^2}\right), \tag{13}$$

$$W_{BC} = -Db_1b_2\left(-\frac{\cos\gamma}{2}\ln\left(\frac{d_1^2d_2^2}{r_c^2(d_1^2-2d_1d_2\cos\gamma+d_2^2)}\right)+\frac{d_1d_2\sin^2\gamma}{d_1^2-2d_1d_2\cos\gamma+d_2^2}\right), \tag{14}$$

where $\gamma = \alpha_1 + \alpha_2$.

Thus, we have all the terms of the total energy density W_1^t of the initial defect configuration (figure 2 (*a*)). The terms are given by equations (2)–(4) and (12)–(14).

The total energy density W_2^t of the final defect configuration (figure 2 (*b*)) resulting from the considered plastic deformation act at triple junction of GBs can be formally written in the form similar to the total energy density W_1^t of the initial defect configuration (see equation (1)), that is through the proper energy densities of dislocation dipoles and the energy densities which characterize their pair interactions. To do this, we need to represent the dislocation with Burgers vector $\mathbf{b}_3$, resulting from the dislocation reaction at triple junction (figure 2 (*b*)), as a superposition of the three dislocations participating in the reaction. This representation will allow us to use equations (2)–(4) and (12)–(14) in their slightly modified forms in the description of terms composing the total energy density W_2^t. In doing this, the key modification of the expressions discussed is in replacing terms that correspond to contributions of cores of the three initial dislocations (figure 2 (*a*)) by a term which describes the corresponding contribution of the resultant dislocation core.

Following the approach considered, the total energy density of the final defect configuration (figure 2 (*b*)) can be written as follows:

$$W_2^t = W_b - \tau b_0 l\cos(2\beta) + W_A^e + W_B^e + W_C^e + W'_{AB} + W'_{AC} + W'_{BC} + \sum_{i=0}^{3} W_i^c. \tag{15}$$

Here W_b denotes the energy barrier for movement of the GB dislocation with Burgers vector $\mathbf{b}_0$ across the central triple junction, β the angle between the GB plane with dipole A and the plane of the shear stress τ action, and W_A^e, W_B^e and W_C^e are the proper elastic energy densities of GB dislocation dipoles A, B and C, respectively. W'_{AB}, W'_{AC} and W'_{BC} are the energy densities that characterize the elastic interactions between dipoles A and B, A and C, and B and C, with transfer of the dislocation of the dipole A taken into account; W_i^c $(i = 0, 1, 2, 3)$ is the core energy density of the ith dislocation with Burgers vector $\mathbf{b}_i$.

The energy barrier W_b for GB dislocation motion is an analogue of Peierls barrier for conventional lattice dislocations. It is caused by atomic configuration at the central triple junction and, in general, represents a structural and material characteristic (which is independent on grain size d). Analysis of its dependence on geometric parameters of the triple junction is beyond the scope of this paper. We focus on the relationship between GB dislocation Burgers vectors, geometric parameters (angles between adjacent GBs) of triple junctions, grain size d and

shear stress τ. Therefore, in the present paper, hereafter we assume W_b (see equations (23) and (26)) to be an adjustable parameter of our model.

The proper elastic energy densities of dislocation dipoles are given by equations (2)–(4) where terms Z_i are removed:

$$W_A^e = Db_0^2 \ln\left(\frac{d_0 + l}{r_{c0}}\right), \tag{16}$$

$$W_B^e = Db_1^2 \ln\left(\frac{d_1}{r_{c1}}\right), \tag{17}$$

$$W_C^e = Db_2^2 \ln\left(\frac{d_2}{r_{c2}}\right). \tag{18}$$

Here $r_{c0} \approx r_{c1} \approx r_{c2} = r_c$.

The energy densities that characterize the elastic interactions between dislocation dipoles are given by equations (12)–(14) with d_0 being replaced by $d_0 + l$. In doing this, we have

$$W'_{AB} = W_{AB}(d_0 \to d_0 + l), \tag{19}$$

$$W'_{AC} = W_{AC}(d_0 \to d_0 + l), \tag{20}$$

$$W'_{BC} = W_{BC}. \tag{21}$$

The dislocation core energy densities in the first approximation are given by the well-known formula (Hirth and Lothe 1982)

$$W_i^c = Db_i^2 Z_i, \quad i = 0, 1, 2, 3. \tag{22}$$

With equations (16)–(22) substituted into equation (15), we find the total energy density W_2^t in the final state of the defect configuration (figure 2 (*b*)). Then the characteristic difference $\Delta W^t = W_2^t - W_1^t$ between the energy densities of the configuration in its final (figure 2 (*b*)) and initial (figure 2 (*a*)) states is as follows:

$$\begin{aligned}\Delta W^t = W_b - \tau b_0 l \cos(2\beta) + D\Bigg\{&\frac{Z}{2}\left(b_3^2 - b_0^2 - b_1^2 - b_2^2\right) + b_0^2 \ln\left(\frac{d_0 + l}{d_0}\right) \\ &+ b_0 \sum_{i=1}^{2}\Bigg[\frac{b_i^2}{2}\cos\alpha_i \ln\left(\frac{d_0^2\left[(d_0 + l)^2 + 2(d_0 + l)d_i\cos\alpha_i + d_i^2\right]}{(d_0 + l)^2(d_0^2 + 2d_0 d_i\cos\alpha_i + d_i^2)}\right) \\ &+ \frac{b_i d_0 d_i \sin^2\alpha_i}{d_0^2 + 2d_0 d_i\cos\alpha_i + d_i^2} - \frac{b_i(d_0 + l)d_i\sin^2\alpha_i}{(d_0 + l)^2 + 2(d_0 + l)d_i\cos\alpha_i + d_i^2}\Bigg]\Bigg\}.\end{aligned} \tag{23}$$

The structure of equation (23) for ΔW^t is evident. The term $(Z/2)(b_3^2 - b_0^2 - b_1^2 - b_2^2)$ describes a change in the sum dislocation core energy due to the dislocation reaction at a triple junction. The term $b_0^2 \ln[(d_0 + l)/d_0]$ specifies the change in the proper energy of dipole A due to transfer of one dislocation composing the dipole by a distance l. The terms in the sum $\sum$ describe changes in the interaction energies associated with the dislocation transfer in question.

The transformation of GB dislocation configuration (figure 2) occurs as an energetically favourable process, if $\Delta W^t < 0$. In this situation, the equation $\Delta W^t = 0$ allows one to obtain the critical shear stress τ_c needed for realization of the transformation. In order to find an analytic relationship between τ_c, dislocation Burgers vectors and geometric parameters of triple junctions, let us first consider the

special case where $d_0 = d_1 = d_2 = d$. In these circumstances, equation (23) is simplified, and the critical shear stress τ_c is found from

$$\tau_c'(d) = p + q\,\frac{l}{d} + s\,\frac{l^2}{d^2}\ , \tag{24}$$

where

$$\tau_c' = \frac{\tau_c}{D}\,b_0 l\cos(2\beta), \tag{25}$$

$$p = \frac{W_b}{D} + \frac{Z}{2}\,(b_3^2 - b_0^2 - b_1^2 - b_2^2), \tag{26}$$

$$q = \frac{b_0}{2}\,(2b_0 - b_1\cos\alpha_1 - b_2\cos\alpha_2), \tag{27}$$

$$s = \frac{b_0}{4}\left[\frac{b_1\sin^2\alpha_1}{(1+\cos\alpha_1)^2} + \frac{b_2\sin^2\alpha_2}{(1+\cos\alpha_2)^2}\right]. \tag{28}$$

In deriving equations (24), (27) and (28), we have used the inequality $l \ll d$ and the relationships $\ln(1 + l/d) \approx l/d$ and $(1 + l/d)^2 \approx 1 + 2l/d$. From figure 2 (*b*) the following relationships can be extracted: $b_0 = b_1\cos\alpha_1 + b_2\cos\alpha_2 + b_3\cos\alpha_3$ and $b_1\sin\alpha_1 = b_2\sin\alpha_2 - b_3\sin\alpha_3$. With these relationships, the second term in equation (26) can be rewritten as

$$b_3^2 - b_0^2 - b_1^2 - b_2^2 = 2b_1b_2\cos(\alpha_1 + \alpha_2) - 2b_0\,(b_1\cos\alpha_1 + b_2\cos\alpha_2). \tag{29}$$

With this formula, all the parameters appearing in equation (24) depend on only the characteristics of the initial defect configuration shown in figure 2 (*a*). The parameter p is always positive, but it may change in a non-monotonic way with variations b_i and α_i (see below). The parameter q is either positive or negative, depending on relationships between b_0 and $b_i\cos\alpha_i$ ($i = 1, 2$). In particular, $q < 0$ at low α_i and large b_i, and $q > 0$ in the opposite case. Values of q (and, as a corrollary, values of τ_c') increase with increasing angles α_i and decreasing b_i. The parameter s is always positive, but the contribution of the term sl^2/d^2 to τ_c (see equation (24)) is always negligibly small.

Thus, in the situation with all grains having the same sizes d, the dependence of the shear stress τ_c (characterizing the GB sliding) on grain size d is given by equation (24) with the two hyperbolic and d^{-2}-type terms sensitive to d. For positive (or negative) values of parameter q, the $1/d$ term gives rise to an increase (or a decrease respectively) in τ_c with reducing grain size d. The d^{-2}-type term with an always positive coefficient s causes an increase in τ_c on a reduction in the grain size d. However, this term commonly is negligibly small (owing to the low l) compared with the hyperbolic term.

With $x = d^{-1/2}$, from equation (24) we have the following dependence which is written in variables used to describe the classical Hall–Petch dependence:

$$\tau_c'(x) = p + qlx^2 + sl^2x^4\ . \tag{30}$$

This formula is convenient in an analysis of the deviations of $\tau_c(d^{-1/2}) = \tau_c(x)$ dependence from the classical Hall–Petch relationship. From equation (30) it follows that there are the two parabolic and x^4-type terms sensitive to $x = d^{-1/2}$. The x^4 term is small and therefore will be hard to detect experimentally, in contrast with the parabolic term. The x^2 term, in the framework of our model, is responsible for the deviations of $\tau_c(d^{-1/2})$ dependence from the classical Hall–Petch relationship.

Now let us consider the general situation where GBs adjacent to the central triple junction have different lengths. To describe this situation, we suppose that $d_i/d_0 = a_i$ $(i = 1, 2)$ and $d_0 = d$. In these circumstances, the first term p in equation (30) does not change, while the parameter q in the second term on the right-hand side of equation (30) has the following form:

$$q(a_1, a_2) = b_0\left(b_0 - b_1\,\frac{a_1\cos\alpha_1(a_1+\cos\alpha_1)}{a_1^2+2a_1\cos\alpha_1+1} - b_2\,\frac{a_2\cos\alpha_2(a_2+\cos\alpha_2)}{a_2^2+2a_2\cos\alpha_2+1}\right). \tag{31}$$

The sign of parameter q given by equation (31) is highly sensitive to the parameters a_i. The third term on the right-hand side of equation (30) is as follows:

$$S(x, a_1, a_2) = b_0\sum_{i=1}^{2}\left(\frac{b_i a_i\sin^2\alpha_i}{a_i^2+2a_i\cos\alpha_i+1} - \frac{b_i a_i\sin^2\alpha_i\,(1+lx^2)}{a_i^2+2a_i\cos\alpha_i(1+lx^2)+(1+lx^2)^2}\right). \tag{32}$$

Thus, in the situation discussed, the critical shear stress that characterizes GB sliding in the framework of our model is represented as

$$\tau_c'(x, a_1, a_2) = p + q(a_1, a_2)lx^2 + S(x, a_1, a_2)\,, \tag{33}$$

here p, $q(a_1, a_2)$ and $S(x, a_1, a_2)$ are given by equations (26), (31) and (32) respectively. This is the main result of our model.

§4. Plastic flow in as-prepared and heat-treated nanocrystalline materials: comparison with experiments

Let us compare the results of our model and experimental data (Volpp *et al.* 1997) on measurements of microhardness H_V in as-prepared and heat-treated nanocrystalline NiAl materials synthesized by the ball-milling technique. In our calculations we shall use the following characteristic values of parameters of these materials and defect configuration under consideration. The elastic constants are (Volpp *et al.* 1997) $G = 70$ GPa and $\nu = 0.314$. For simplicity of analysis, we assume that $\alpha_1 = \alpha_2 = \alpha$, $Z = 1$ and $\beta = 0$. Moduli of the GB dislocation Burgers vector are taken as follows: $b_0 = 0.1$ nm and $b_1 = b_2 = 0.08$ nm (in other terms, $a/5$ and $a/3$, with a being the crystal lattice parameter); they correspond to those of experimentally observed GB dislocations (Sutton and Balluffi 1995). The distance by which the GB dislocation with Burgers vector $\mathbf{b}_0$ moves is $l = 1$ nm; it corresponds to the characteristic thickness of GBs. These values are considered reasonable based on the information available. As we shall see later, the actual forms of the predicted curves are not too sensitive on their values. The energy barrier for GB dislocation motion is assumed to be $W_b = \xi G b_0^2$, where ξ is the adjusting parameter being of the order of unity. This formula is written empirically as a typical 'dislocation energy' term. Its dimension and order of magnitude are those of the core energy of dislocation. Also to compare theoretical calculations of the yield stress τ_c with experimental measurements of the microhardness H_V^{th}, we shall use the known relationship (Tabor 1951) $H_V^{th} \approx 3\sigma_y(\varepsilon = 8\%) \approx 6\tau_y$.

Equation (33) predicts the relation between yield stress and grain size provided that the mechanism described in the paper is dominant. To compare this result with experiments, especially with those of Volpp *et al.* (1997), we proceed by noting that the last term, that is, $S(x, a_1, a_2)$, can be safely neglected, as mentioned before.

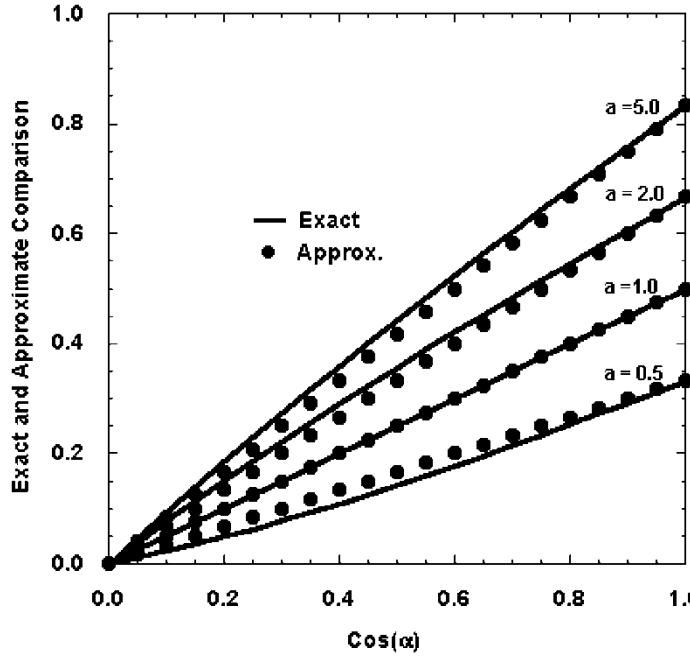

Figure 3. Comparison of two terms in equation (34). (See text for explanation).

The term $q(a_1, a_2)$ can in principle be both positive and negative as given by equation (31). It is easy to show that, for the range of $\cos\alpha$,

$$\frac{a\cos\alpha\,(a+\cos\alpha)}{a^2+2a\cos\alpha+1} \approx \frac{a}{a+1}\cos\alpha. \tag{34}$$

In figure 3, we compare these two terms and show how close the two terms are for the several values of a.

Therefore $q(a_1, a_2)$ can be written as

$$q(a_1, a_2) = b_0\left(b_0 - b_1\cos\alpha\frac{a_1}{a_1+1} - b_2\cos\alpha\frac{a_2}{a_2+1}\right). \tag{35}$$

The term $(a\cos\alpha)/(a+1)$ can at most be equal to one and, if $a \approx 1$ (grain sides approximately equal), then it is $\frac{1}{2}$ or less. Next we note that the angle α will not always be close to zero but may vary from 0 to $\pi/2$. Therefore this term on averaging over α will be $2/\pi$ or less which is 0.637 or less, whatever the value of a. More simply, one notes that $\frac{1}{2} < a/(a+1) < 1$ and $0 < \cos\alpha < 1$ which gives average $a/(a+1) \approx \frac{3}{4}$ and, if $\cos\alpha \approx \frac{1}{2}$, then $(a\cos\alpha)/(a+1) \approx \frac{3}{8}$. Therefore, if we take $b_0 = 0.1\,\text{nm}$ and $b_1 = b_2 = 0.08\,\text{nm}$ as previously stated, there is a very good possibility that $q(a_1, a_2)$ is positive, especially if a_1 and a_2 are not too large.

We shall therefore assume that $q(a_1, a_2)$ is positive and then apply the procedure given by Masumura *et al.* (1998) for averaging over the grain size distribution to develop a yield stress – (average grain size)$^{-1/2}$ curve to take into account the range of grain sizes in a nanocrystalline material. This is done by assuming that the mechanism discussed in the present paper operates for grain sizes less than d^*,

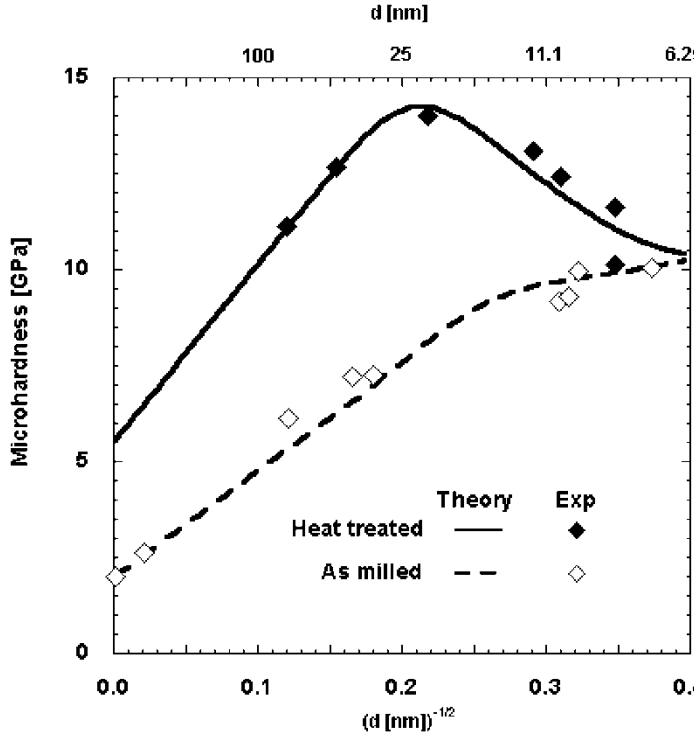

Figure 4. Comparison of theoretical predictions with the experimental results of Volpp *et al.* (1997).

and the usual Hall–Petch mechanism operates for grain sizes higher than d^*. The statistical nature of the grain sizes in a polycrystal is taken into consideration by using an analysis similar to that employed by Kurzydlowski (1990). The volumes of the grains are assumed to be log-normally distributed, and the standard deviation of the distribution was taken to be 1. Figure 4 gives the full curve following this procedure for the whole range of average grain sizes where d^* was taken as 16 nm. The curve then needs the value of a single parameter λ given by ql/pd^*. The best fit is obtained for $\lambda = 0.10$, which corresponds to $q/p = 1.6$ if l is taken to be 1 nm. This ratio appears to be reasonable but cannot yet be calculated exactly, because of the uncertainty in the values of the parameters needed to calculate p and q.

Next we discuss the specific features of plastic deformation in annealed nanocrystalline materials. The heat treatment causes annihilation of GB dislocations, carriers of GB sliding, which gives rise to the hampering of GB sliding. In fact, the generation of new GB dislocations commonly requires intensive flows of lattice dislocations from grain interiors to GBs, where lattice dislocations split into GB dislocations. At the same time, the density of lattice dislocations is low in annealed materials, while their nucleation under mechanical load is hampered owing to nanoscale effects (for details, see Gryaznov *et al.* (1991) and Romanov (1995)). Since GB sliding is suppressed, deformation mechanisms alternative to GB sliding are capable of effectively contributing to plastic flow or even being dominant in such materials. In the context discussed, the case of the annealed nanomaterial used by Volpp *et al.* (1997) can also be explained. In this case, however, the mechanism

proposed by Masumura *et al.* (1998), based on the idea that at least for very small well annealed grains Coble-creep type behaviour may be applicable, holds. It was also postulated that modelling of strengthening by nanocrystalline materials needs consideration of both dislocation interactions and sliding due to Coble creep acting simultaneously if the polycrystals have a distribution in sizes as is always the case. Their model is thus based on using Coble creep (with a threshold stress) for finer grains and conventional Hall–Petch strengthening for larger grains incorporating into the analysis to a distribution of grain sizes occurring in most specimens. In the Masumura *et al.* (1998) model the τ versus d relationship used for Coble creep is given by

$$\tau_c = \frac{A}{d} + Bd^3, \tag{36}$$

where B is as usual both a temperature- and a strain-rate dependent constant as given by Masumura *et al.* (1998). This threshold term A/d can be large if d is in the nanometre range. We again denote by d^* the grain size at which a transition from dislocation mode to Coble creep mode happens. So d^* is now given by

$$k(d^*)^{-1/2} = \frac{A}{d^*} + B(d^*)^3. \tag{37}$$

It is likely that the transition from dislocation mode to other modes happens at around the same grain size and d^* should be taken the same for both types of specimen.

The dislocation mode of deformation (i.e. for large grains) is common to both types of specimen and this mode depends only on the grain size; hence it is reasonable to assume that a transition from dislocation mode to other modes will occur at a fixed value of grain size irrespective of deformation modes at smaller grain sizes. (We tried to use two different grain sizes for two cases and found that the agreement with experimental data plotted in figure 4 was not improved.)

For completeness we apply the procedure given by Masumura *et al.* (1998) and we show this result also in figure 4. For this case we also take $d^* = 16$ nm and a value of 0.13 for P, the ratio of Coble threshold stress to the conventional stress; that is,

$$P = \frac{A/d^*}{B(d^*)^3}. \tag{38}$$

Thus both the curves can be satisfactorily explained at least approximately. Our analysis thus points to two different mechanisms operating for the finer grains, and a common dislocation mechanism operating for the larger grains in the two types of specimen studied by Volpp *et al.* (1997).

The values of λ and P used for comparison, although reasonable, need further investigation.

§ 5. Discussion and concluding remarks

Thus, according to the results of our theoretical analysis, the yield stress characterizing GB sliding in nanocrystalline materials is caused by transformations of GB dislocations at triple junctions (figure 2). In doing this, the grain size and geometry of triple junctions strongly influence the GB sliding as a channel of plastic deformation. In particular, GB dislocations overcome easily a triple junction of GBs, if its characteristic abutting angles α_1 and α_2 are small enough. With a high density

of GB dislocations and 'soft' triple junctions (with small α_1 and α_2) in as-prepared nanocrystalline materials, GB sliding intensively occurs in these materials where it effectively competes with the conventional dislocation slip highly sensitive to grain size. In order to describe the competition between the conventional dislocation slip and GB sliding, we have taken into consideration the grain size d and triple junction angle α distributions, accounting for such distributions that occur in real specimens. With these distributions, the yield stress dependence on grain size in as-prepared materials, calculated in the framework of our model, is in rather good agreement with the corresponding experimental data (Masumura *et al.* 1998) on mechanical characteristics of as-prepared nanocrystalline NiAl materials synthesized by the ball milling technique (see figure 4).

Heat treatment of nanocrystalline materials gives rise to annihilation of GB dislocations and causes triple junctions to be mostly at equilibrium, that is those characterized by abuting angles of about 120°. These structural transformations suppress GB sliding, in which case alternative deformation mechanisms associated with the active role of GBs compete with conventional dislocation slip in heat-treated nanocrystalline materials. Here, following the approach by Masumura *et al.* (1998), we have calculated the yield stress dependence on grain size d in heat-treated nanocrystalline NiAl materials, taking into account competition between the conventional dislocation slip and Coble creep (treated to be alternative to GB sliding). The theoretical dependence again is in a good agreement with the corresponding experimental data (Volpp *et al.* 1997).

The annealing of the specimen will definitely affect the long-range order and vacancy concentration. This is taken into account in the two constants A and B. In the calculation only their ratio is needed and this is a parameter whose value is assumed (see equation (38)). The mechanical behaviour of the specimen depends on this parameter, as seen in figure 4.

It is usually believed that GB dislocations can have multiple small Burgers vectors or, in many cases, they seem to be essentially continuous infinitesimal dislocations. However, continuous infinitesimal dislocations are, in fact, a mathematical abstraction only which is used sometimes to simplify treatment of real discrete dislocations (including GB dislocations) or to model some special stress (strain) distributions, in contrast with the more realistic discrete dislocations that we use in our model. The magnitudes of GB dislocation Burgers vectors, used in our theoretical analysis, are 0.08 and 0.1 nm (or, in other terms, $a/5$ to $a/3$, with a being the crystal lattice parameter); they correspond to those of experimentally observed GB dislocations (for example Sutton and Balluffi (1995)). The functional form of our result does not depend critically on the actual magnitude of these Burgers vectors.

In our treatment we do not consider the piling up of GB dislocation at the triple junction. In principle, real discrete dislocations can form pile-ups near triple junctions of GBs. Then the dislocation distribution between triple points will represent a pile-up dipole with a complex reaction at the tip. However, the formation of a GB dislocation pile-up near a triple junction needs a certain level of external stress (considered, for example, in the paper by Fedorov *et al.* (2003)) which is usually much higher than the stress which is necessary to form a dipole of discrete dislocations. This is why we consider dipoles of discrete dislocations in our model. We consider the lowest possible stress that is necessary to apply to make a dislocation pass through the triple junction. Namely this stress is identified with 'yield stress' in

our paper. In this context, we show that under this stress even a single dislocation can bypass the triple junction. It is difficult to see how this triple junction would be an obstacle to a whole array of discrete dislocations forming a dislocation pile-up. Our result conclusively proves there will be no pile-ups under these conditions at the triple junctions.

We are of course not asserting that pile-ups at the triple junctions never exist. We think that there exist two possible situations whose realization depends on the strength of a triple junction.

(i) The triple junction strength is sufficiently low for the stress that is needed for dislocation bypass through the junction to also be low, and even lower than that which is necessary to create a dislocation pile-up.
(ii) The triple junction strength is sufficiently high to provide formation of a dislocation pile-up before the head dislocation will bypass through the junction.

In our model we deal with case (i) only because we consider as-sintered nanomaterials, which are expected to contain triple junctions of different strengths: low and high. Of course, we have had to consider 'weak links' to estimate the yield stress. Hence the discrete dipole process analysed by us here is expected to be more realistic.

Finally we note that the stress fields of the triple junction itself has been neglected in our treatment. A detailed consideration of stress fields is not required for the problem under consideration. It would be required if we were considering in detail the atomic structure of the triple junction or at least considering an anisotropic continuum model. Our isotropic model is focused on the yield stress dependence on grain size d, in which case a complicated and space-consuming description of the atomic structure of the triple junction is not needed. Instead we use the concept of an energy barrier due to the triple junction in our isotropic model, which as we show is enough to capture the basic aspects related to the yield stress dependence on the grain size d.

It is worth noting that, during the last decade, many researchers have tried to explain the peculiarities of Hall–Petch curves for nanostructured materials. The existing theoretical models may be subdivided into two types. The models of the first type are based on using a 'rule-of mixtures' approach (Gryaznov *et al*. 1993, Carsley *et al*. 1995, Milligan *et al*. 1995, Wang *et al*. 1995, Ovid'ko 1997, Kim 1998, Konstantinidis and Aifantis 1998, Song *et al*. 1999, Kim *et al*. 2000) while those of the second type involve specific physical mechanisms of dislocation plasticity as piling of lattice dislocations near GBs (Lian *et al*. 1993, Nazarov 1996, Pande and Masumura 1996), their absorption by GBs (Malygin 1995), penetration through the boundaries (Lu and Sui 1993), interaction with GB dislocations (Seattergood and Koch 1992) or with triple junction disclinations (Zaichenko and Glezer 1997). We have recently given a review of these models (Gutkin *et al*. 2001) where it was shown that most of them are in good accordance with experimental data. On the other hand, many of them are restricted by the range of large grain sizes where lattice dislocation motion still dominates over other mechanisms of plasticity or by very severe assumptions, for example about the amorphous nature of GBs in nanocrystalline metals. In elaborating our present model, we have tried to avoid such strong restrictions by using the grain-size distribution approach (Masumura *et al*. 1998, Fedorov *et al*. 2002) which allows us to include both the bulk lattice (for larger grains) and the GB (for smaller grains) mechanisms of plasticity.

To summarize, the idea of competition between conventional dislocation slip and deformation modes associated with active role of GBs (GB sliding and Coble creep) in nanocrystalline materials effectively describes experimentally detected deviations of the yield stress dependence on grain size at small grains. In doing this, according to the results of our theoretical model, GB sliding dominates in as-prepared nanocrystalline materials where densities of GB dislocations and soft triple junctions are rather high. Coble creep (diffusional creep associated with enhanced diffusion along GBs) crucially contributes to plastic flow in heat-treated nanocrystalline materials where the density of GB dislocations (carriers of GB sliding) is low and triple-junction geometry predominantly hampers GB sliding.

Acknowledgements

This work was supported, in part (for M.Yu.G. and I.A.O.), by the 'Integration' Program (grant B0026), (for M.Yu.G.) by the Russian State Research Program on Solid-State Nanostructures, and (for I.A.O.) by the Office of US Naval Research (grant N00014-01-1-1020), Russian Academy of Sciences (RAS) Program 'Structural mechanics of materials and constructions' and the Russian Foundation of Basic Researches (grant 01-02-16853).

References

Carsley, J. E., Ning, J., Milligan, W. W., Hackney, S. A., and Aifantis, E. C., 1995, *Nanostruct. Mater.*, **5**, 441.

Fedorov, A. A., Gutkin, M. Yu., and Ovid'ko, I. A., 2002, *Scripta mater.*, **47**, 51; 2003, *Acta mater.*, **51**, 887.

Gryaznov, V. G., Gutkin, M. Yu., Romanov, A. E., and Trusov, L. I., 1993, *J. Mater. Sci.*, **28**, 4359.

Gryaznov, V. G., Polonsky, I. A., Romanov, A. E., and Trusov, L. I., 1991, *Phys. Rev.* B, **44**, 42.

Gutkin, M. Yu., and Ovid'ko, I. A., 1994, *Phil. Mag.* A, **70**, 561; 2001, *Phys. Rev.* B, **63**, 064 515.

Gutkin, M. Yu., Ovid'ko, I. A., and Pande, C. S., 2001, *Rev. Adv. Mater. Sci.*, **2**, 80.

Gutkin, M. Yu., Kolesnikova, A. L., Ovid'ko, I. A., and Skiba, N. V., 2002, *Phil. Mag. Lett.*, **81**, 651.

Hackney, S. A., Ke, M., Milligan, W. W., and Aifantis, E. C., 1996, *Processing and Properties of Nanocrystalline Materials*, edited by C. Suryanarayana, J. Singh and F. H. Froes (Warrendale, Pennsylvania: Metallurgical Society of AIME), pp. 421–426.

Hahn, H., Mondal, P., and Padmanabhan, K. A., 1997, *Nanostruct. Mater.*, **9**, 603.

Hahn, H., and Padmanabhan, K. A., 1997, *Phil. Mag.* B, **76**, 559.

Hirth, J. P., and Lothe, J., 1982, *Theory of Dislocations* (New York: Wiley).

Ke, M., Hackney, S. A., Milligan, W. W., and Aifantis E. C., 1995, *Nanostruct. Mater.*, **5**, 689.

Kim, H. S., 1998, *Scripta. Mater.*, **39**, 1057.

Kim, H. S., Estrin, Y., and Bush, M. B., 2000, *Acta Mater.*, **48**, 493.

King, A. H., 1999, *Interface Sci.*, **7**, 251.

Koch, C. C., Morris, D. G., Lu, K., and Inoue, A., 1999, *Mater. Res. Soc. Bull.*, **24**, 54.

Konstantinidis, D. A., and Aifantis, E. C., 1998, *Nanostruct. Mater.*, **10**, 1111.

Kurzydlowski, K. J., 1990, *Scripta. metall. mater.*, **24**, 879.

Lu, K., and Sui, M. L., 1993, *Scripta. metall. mater.*, **28**, 1465.

Lian, J., Baudelet, B., and Nazarov, A. A., 1993, *Mater. Sci. Engng*, **A172**, 23.

Malygin, G. A., 1995, *Phys. Solid St.*, **37**, 1248.

Masumura, R. A., Hazzledine, P. M., and Pande, C. S., 1998, *Acta mater.*, **46**, 4527.

Milligan, W. W., Hackney, S. A., and Aifantis, E. C., 1995, *Continuum Models for Materials with Microstructure*, edited by H. B. Mühlhaus (New York: Wiley), pp. 379–393.

Mohamed, F. A., and Li, Y., 2001, *Mater. Sci. Engng*, **A298**, 1.
Mura, T., 1968, *Adv. Mater. Res.*, **3**, 1.
Murayama, M., Howe, J. M., Hidaka, H., and Takaki, S., 2002, *Science*, **295**, 2433.
Nazarov, A. A., 1996, *Scripta. Mater.*, **34**, 697.
Ovid'ko, I. A., 1997, *Nanostruct. Mater.*, **8**, 149; 2002, *Science*, **295**, 2386.
Owusu-Boahen, K., and King, A. H., 2001, *Acta mater.*, **49**, 237.
Padmanabhan, K. A., 2001, *Mater. Sci. Engng*, **A304–A306**, 200.
Pande, C. S., and Masumura, R. A., 1996, *Processing and Properties of Nanocrystalline Materials*, edited by C. Suryanarayana, J. Singh and F. H. Froes (Warrendale, Pennsylvania: Metallurgical Society of AIME), p. 387.
Rabukhin, V. B., 1986, *Poverkhnost*, **7**, 126.
Romanov, A. E., 1995, *Nanostruct. Mater.*, **6**, 125.
Seattergood, R. O., and Koch, C. C., 1992, *Scripta Mater.*, **27**, 1195.
Song, H. W., Guo, S. R., and Hu, Z. Q., 1999, *Nanostruct. Mater.*, **11**, 203.
Sutton, A. P., and Balluffi, R. W., 1995, *Interfaces in Crystalline Materials* (Oxford: Clarendon).
Tabor, D., 1951, *The Hardness of Metals* (Oxford University Press), p. 107.
Valiev, R. Z., and Alexandrov, I. V., 2000, *Nanostructured Materials Prepared by Severe Plastic Deformation* (Moscow: Logos) (in Russian).
Volpp, T., Göring, E., Kuschke, W.-M., and Arzt, E., 1997, *Nanostruct. Mater.*, **8**, 855.
Wang, N., Wang, Z., Aust, K. T., and Erb, U., 1995, *Acta metall. mater.*, **43**, 519.
Weertman, J. R., and Sanders, P. G., 1994, *Solid St. Phenomena*, **35–36**, 249.
Yamakov, V., Wolf, D., Phillpot, S. R., and Gleiter, H., 2002, *Acta mater.*, **50**, 61.
Zaichenko, S. G., and Glezer, A. M., 1997, *Phys. Solid St.*, **37**, 1810.